

A study of 60 GHz channel estimation techniques using pilot carriers in OFDM systems in a confined area

Ahmad El Assaf, Nahi Kandil, Nadir Hakem
LRTCS Laboratory
450, 3e Ave, Val-d'Or,
Quebec, Canada, J9P 1S2
Email: (Ahmad.el-assaf, Nahi.Kandil,
Nadir.Hakem) @uqat.ca

Sofiène Affès
INRS-EMT,
800, de la Gauchetière West,
Suite 6900, H5A 1K6
Email: affes@emt.inrs.ca

Paul Fortier
ECE Department, Laval University
Quebec, Quebec, Canada,
G1V 0A6
Email: paul.fortier@gel.ulaval.ca

Abstract—In recent years, there has been an increased need for digital wireless applications to use high rate data transmission. OFDM (Orthogonal Frequency Division Multiplexing) offers an interesting solution that allows for the exploitation of the 60 GHz band with optimal spectral efficiency, a robustness to frequency selective fading, and a resistance to inter-symbol interference (ISI) that is a major problem in high speed data communications. Transmitted data in an OFDM system is divided on different subcarriers, after applying PSK (phase shift keying) or QAM (Quadrature Amplitude Modulation) modulation. The bandwidth of the obtained signal is converted to the time domain by using an IFFT (Inverse Fast Fourier Transform) in order to transmit it through a wireless channel. To recover the distorted data at the receiver, the effects of the channel must be estimated and compensated by the receiving system [1, 2]. In this paper, the 60 GHz channel estimation methods for OFDM systems based on comb-type pilot arrangement are investigated, as the algorithm of channel estimation based on comb-type is divided into pilot signal estimation and channel interpolation. The pilot signal estimation based on LS (Least Squares) or LMMSE (Linear Minimum Mean Square Error) criteria is studied along with the channel interpolation based on LI (linear interpolation). The performances of various estimation algorithms are evaluated and compared by measuring the Bit Error rate (BER) and Mean Square Error (MSE) where 16-QAM modulation scheme is applied.

Keywords: Channel estimation, 60 GHz, OFDM, IEEE802.15.3c, TSV channel model, LS estimation, LMMSE estimation, pilot aided, comb-type.

I. INTRODUCTION

Lately, Orthogonal Frequency Division Multiplexing (OFDM) has received much interest in the field of mobile communications because in wide-band mobile communication systems, the radio channel is usually frequency selective and time varying. This is especially true in a multi-path channel that has a frequency response that is not flat and has faint echoes and reflections of the transmitted signal due to obstacles. Therefore, the transmission environment and transmitted signal propagating via a multi-path channel causes inter-symbol interference (ISI). The ISI may distort the received signal so severely that the transmitted symbols

may not be recovered. Given that channel estimation is an important issue for coherent OFDM systems [3], an effort to develop an appropriate channel estimation and compensation algorithm is necessary.

The channel estimation techniques based on pilot symbols (a reference signal known to both transmitter and receiver) are called Pilot Symbol Assisted Modulation (PSAM). Depending on the arrangement of pilots, different types of pilot structures are referred to as block-type and comb-type.

The first structure, block-type pilot channel estimation, has been developed under the assumption of a slow fading channel. The structure is made by inserting pilot tones into all of the subcarriers of OFDM symbols with a specific period. Whereas the second structure, comb-type pilot channel estimation, has been introduced to satisfy the need for estimation when the channel changes even in one OFDM block [4]. The structure of this pilot type is made by inserting pilot tones into each OFDM symbols. The channel estimation based on comb-type is divided in two steps: the first step estimates the channel frequency coefficients at the pilot symbol positions using LS and LMMSE estimators; the second step interpolates the channel frequency coefficients that correspond to the data symbols using the estimates of the channel frequency coefficients. This study examines the channel interpolation based on linear interpolation.

The paper is organized as follows: In Section II, the OFDM system is described with an explanation of the OFDM's different components of a transmission chain; Section III is dedicated to the 60 GHz channel model; Section IV discusses the two types of pilot arrangements, block-type and comb-type, as well as the channel estimation algorithms LS and LMMSE; Section V presents the simulation parameters and results using MATLAB programming, indicating the BER and MSE improvements; and lastly, the study concludes with Section VII.

II. SYSTEM DESCRIPTION

The OFDM system based on pilot channel estimation is depicted in Figure 1. First, we have the generator of the data that will be transmitted as binary data $b[i]$ of duration T_b . Then, the M-QAM modulator (QAM Mapping) transforms the binary data $b[i]$ in complex symbols $X(k)$ of duration $T_q = \log_2(M.T_b)$ with $M = 4, 16, 64$. After that, the complex symbols $X(k)$ are grouped by passing them through a serial-to-parallel (S/P) converter to generate parallel streams into blocks of N symbols.

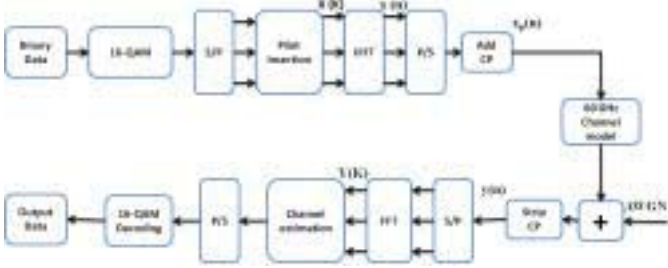


Fig. 1. OFDM system model

Pilot signals (tones) are uniformly inserted into all symbols. The Inverse Fast Fourier Transform (IFFT) block is then used to implement OFDM, which transforms the data sequence $X(k)$ of length N into a complex time-domain signal with the following equation:

$$\begin{aligned} x(n) &= \text{IFFT} \{X(k)\} \\ &= \sum_{k=0}^{N-1} X(k) e^{j2\pi \frac{kn}{N}} \end{aligned} \quad (1)$$

where N is the IFFT length, and $n = 0, 1, 2, \dots, N-1$

In order to reduce the effect of multipath induced ISI, it is possible to use a guard interval or cyclic prefix (CP) as shown in Figure 2. However, for the guard interval to be effective, its duration must be at least equal to or larger than the maximum delay spread of the channel. The insertion of a guard interval between two successive OFDM symbols eliminates inter-carrier interference (ICI). As shown in Figure 2, the CP copies the N_g rear part of the OFDM symbol and puts it in front of the symbol, so the period will increase from T_u to $T_u + T_g$, where T_g is the CP period. We finally obtain the OFDM symbol which contains $N_s = N + N_g$ symbols with total duration equal to $T_s = T_u + T_g$, where N_g is the length of the guard interval.

The resultant OFDM symbol is given as follows:

$$x_p(n) = \begin{cases} x(N+n), & n = -N_g, N_g+1 \dots -1 \\ x(n), & n = 0, 1, \dots, N-1 \end{cases} \quad (2)$$

Now the signal $x_p(n)$ is ready for transmission through the 60 GHz channel with additive noise.

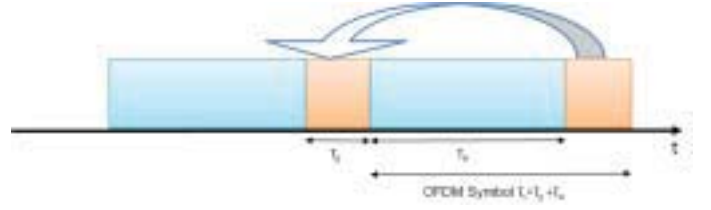


Fig. 2. OFDM symbol structure with a Cyclic Prefix (CP).

The received signal is given by:

$$y_p(n) = x_p(n) \otimes h(n) + w(n) \quad (3)$$

where $h(n)$ is the channel impulse response, $w(n)$ is additive white Gaussian noise (AWGN), and \otimes denotes circular convolution.

Thus, as the signal in the receiver is passed through S/P, we then remove the cyclic prefix from each received symbol to obtain $y(n)$. In this case, the first N_g symbols that contain the interference between the blocks are removed. Afterwards, we begin to apply the FFT module using following operation:

$$\begin{aligned} Y(k) &= \text{FFT} \{y(n)\} \\ &= \frac{1}{N} \sum_{n=0}^{N-1} y(n) e^{-j2\pi \frac{kn}{N}} \end{aligned} \quad (4)$$

where $k = 0, 1, 2, \dots, N-1$.

From equation (4) we can write $Y(k)$ as follows:

$$Y(k) = X(k) \cdot H(k) + W(k) \quad (5)$$

where $k=0, 1, 2, \dots, N-1$.

In summary, the use of the cyclic prefix converts the traditional linear convolution into a circular convolution, which results in the presence of a circulating matrix in the model of the received signal.

Following the FFT block, the pilot signals are extracted from $Y(k)$. With the knowledge of the estimated channel response $\hat{H}(k)$, the estimated transmitted data sample $\hat{X}(k)$ can be recovered simply by dividing the received signal by the estimated channel response.

$$\hat{X}(k) = \frac{Y(k)}{\hat{H}(k)} \quad (6)$$

Finally, the source binary information data are demodulated and reconstructed at the receiver output.

III. CHANNEL MODEL

The need for broadband wireless transmission for 4th generation systems requires a frequency band with high capacity, and the 60 GHz band could be the favorable choice for now. The 60 GHz band is basically a millimeter wave band, which has advantages in the field of mobile broadband communications, and will be therefore exploited to provide

both flexibility and mobility for the new system.

So in the design of communication systems, it is necessary to construct mathematical models that characterize the propagation medium. Our channel model is based on the Triple S-V model, which is a combination of the SV model [5] and the two path model. The SV model does not consider the angle of arrival (AOA), while the TSV channel model considers the AOA. A typical TSV channel model realization is shown in Figure 3.

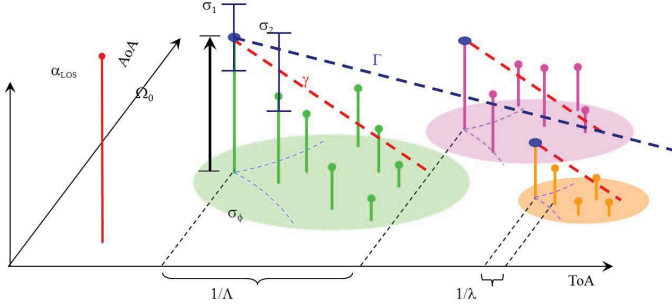


Fig. 3. A typical TSV channel model realization.

The channel impulse response of this model is given by the following equation:

$$h(t, \phi, \theta) = \beta \delta(\tau, \phi, \theta) + \sum_{l=0}^L \sum_{k=0}^{K_l} \alpha_{k,l} \delta(t - T_l - \tau_{k,l}) \delta(\phi - \Omega_l - \omega_{k,l}) \delta(\theta - \Psi_l - \psi_{k,l}) \quad (7)$$

where:

- t represents the time [ns];
- l is the cluster index;
- k is the ray index (within the l -th cluster);
- L is the total number of clusters.
- K_l is the total number of rays in the l -th cluster.
- $\delta(\cdot)$ is the Dirac function.
- T_l is the time of arrival of the first ray in the l -th cluster.
- $\alpha_{k,l}$ denotes the complex amplitude.
- $\tau_{k,l}$ is the time of arrival (ToA) of the k -th ray of the l -th cluster.
- $\omega_{k,l}$ is the angle of arrival (AoA) of the k -th ray of the l -th cluster.
- $\psi_{k,l}$ is the angle of departure (AoD) of the k -th ray of the l -th cluster.
- T_l represents the mean ToA of the l -th cluster.
- Ω_l represents the mean AoA of the l -th cluster.
- Ψ_l represents the mean AoD of the l -th cluster.

The first term, $\beta \delta(\tau, \phi, \theta)$, accounts for the gain of the strict LOS component (i.e. the multipath gain of the first arrival path) which can be found deterministically using ray tracing or a simple geometry based method or statistically [6].

The cluster arrival and ray arrival time distributions are described by two Poisson processes. According to this model, cluster inter-arrival times and ray intra-arrival times are given by two independent exponential pdfs. In particular, the cluster arrival time for each cluster is an exponentially distributed random variable conditioned on the cluster arrival time of the previous cluster, which can be expressed as [6]:

$$p(T_l|T_{l-1}) = \Lambda[-\Lambda \exp(T_l - T_{l-1})] \quad \text{for } l > 0, \quad (8)$$

where Λ is the cluster arrival rate. Similarly, the ray arrival time for each ray is an exponentially distributed random variable conditioned on the ray arrival time of the previous ray given by:

$$p(\tau_{k,l}) = \lambda[-\lambda \exp(\tau_{k,l}|\tau_{k-1,l})] \quad \text{for } k > 0,$$

where λ is the ray arrival rate. The distribution of the cluster mean AoA, Ω_l , conditioned on the first cluster mean AoA, Ω_0 , can be described by a uniform distribution over $[0, 2\pi]$, that is:

$$P(\Omega_l/\Omega_0) = \frac{1}{2\pi}, \quad \text{for } l > 0. \quad (10)$$

Note that the cluster AoA represents the mean of all AoAs within the cluster. On the other hand, the ray AoAs within each cluster can be modeled either by a zero-mean Gaussian distribution or a zero-mean Laplacian distribution which is given by:

$$p(\omega_{k,l}) = \frac{1}{\sqrt{2}\sigma_\phi} \exp\left(-\left|\frac{\sqrt{2}\omega_{k,l}}{\sigma_\phi}\right|\right) \quad (11)$$

IV. CHANNEL ESTIMATION TECHNIQUES

In this section, we describe the channel estimation techniques based on pilot symbols. This method uses the symbols known to both transmitter and receiver in order to make an estimation. The attenuation of pilot symbols is measured and the data symbols between the pilot symbols are interpolated. According to the literature, there are two major pilot classes, defined by the arrangement of pilot insertion: block-type arrangement and comb-type arrangement [3, 4]. In general, there are two principles of OFDM channel estimation, least squares (LS) and the linear estimator with minimum Mean Square Error (LMMSE). The LS estimator is currently used in OFDM systems due to its simple application and low complexity. However, the influence of noise is not taken into account in the LS estimator. Instead, the LMMSE estimator is more precise than the LS estimator, as noise is taken into account in LMMSE calculations.

A. Block type arrangement

The block-type arrangement is shown in Figure 4. The block-type pilot is developed under the assumption of a slow fading channel.

In this type, the pilot tones are inserted into all subcarriers of OFDM symbols with a specific period in time, S_t , that

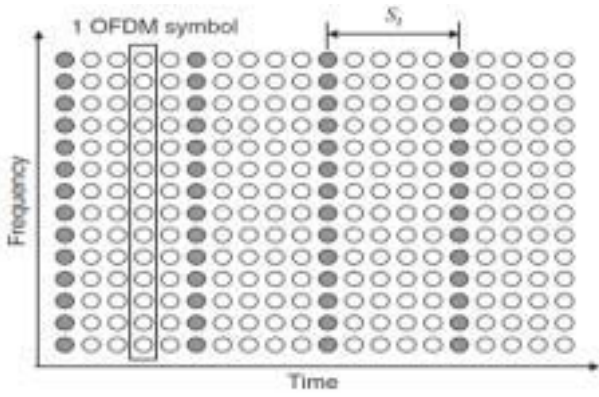


Fig. 4. Block-type pilot arrangement.

must be smaller than the coherence time of the channel.

As the coherence time is given in an inverse form of the Doppler frequency f_D in the channel, the pilot symbol period must satisfy the following inequality:

$$S_t \leq \frac{1}{f_D} \quad (12)$$

B. Comb-type arrangement

The block-type arrangement is shown in Figure 5. The comb-type pilot channel estimation is introduced to satisfy the need for equalizing when the channel changes even from one OFDM block to the subsequent one.

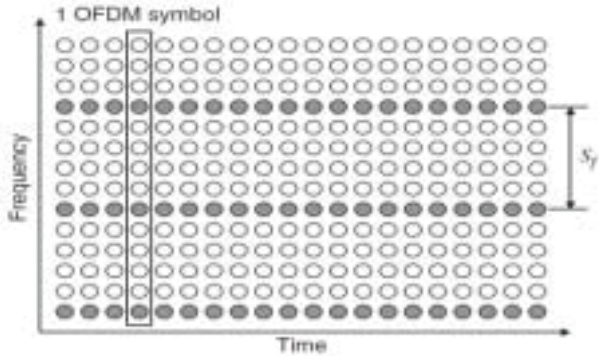


Fig. 5. Comb-type pilot arrangement.

In this type, the pilot symbols are sent on some sub-carriers continuously and the channel characteristics are always known, but for just a few carrier frequencies with a spacing of pilots symbols S_f that must be much smaller than the coherence bandwidth of the channel, B_c . As the coherence bandwidth is determined by the inverse of the maximum delay spread, σ_{\max} , the period of pilot symbol must satisfy the following inequality:

$$S_f \leq \frac{1}{\sigma_{\max}} \quad (13)$$

C. LS Estimator

As an estimator, LS is a statistic that considers the values close to the unknown value of the parameter. The technique of LS channel estimator assesses the channel without considering noise characteristics. So, as seen in Section II, the received signal at the output of the FFT can be written in the following matrix form: $Y = XH + W$. Let $W = (Y - XH)$ and $J = E\{W^{\#}W\}$ the correlation matrix of W , where superscript or exponent denote matrix hermitian. Since the objective of the algorithm LS is to minimize the parameter J , that means it is another way to minimize the factor $(Y - XH)(Y - XH)^{\#}$. Consequently, the LS estimate is represented by the following equation:

$$\hat{H}_{LS} = \frac{Y}{X} = Y.X^{-1} \quad (14)$$

D. LMMSE ESTIMATOR

The linear minimum mean square error (LMMSE) minimizes the mean square error (MSE) between the actual and estimated channel coefficients using the channel frequency correlation. This is achieved by a linear transformation applied to the optimal LS estimator described in the previous section. The LMMSE estimator is given by:

$$\hat{H}_{LMMSE} = R_{HH} \left(R_{HH} + \sigma_n^2 (XX^{\#})^{-1} \right)^{-1} \hat{H}_{LS} \quad (15)$$

We denote by σ_n^2 is the variance of AWGN, and R_{HH} is the auto covariance matrix of the channel given by:

$$R_{HH} = E\{W^{\#}W\} \quad (16)$$

In (15), the calculation of $(XX^{\#})^{-1}$ involves high complexity. To reduce this complexity, it is possible to replace the term $(XX^{\#})^{-1}$ in this equation with its expectation, $E\{(XX^{\#})^{-1}\}$. Then (15) can be rewritten as:

$$\hat{H}_{LMMSE} = R_{HH} \left(R_{HH} + \frac{\beta}{SNR} I \right)^{-1} \hat{H}_{LS} \quad (17)$$

where β is $E\{|X_k|^2\}E\{\left|\frac{1}{X_k}\right|^2\}$, and SNR is defined as $\frac{E\{|X_k|^2\}}{\sigma_n^2}$. β is set by the modulation constellation.

V. SIMULATION RESULTS AND ANALYSIS

In this section, comparisons are performed among LS and LMMSE channel estimations for different conditions of channel that includes the LOS and NLOS cases. The simulation parameters are shown in Table 1. In our simulation, CM1, CM3, and CM4 are adopted, which are respectively based on line-of-sight (LOS) and non-line-of-sight (NLOS), where CM1 represents a residential LOS environment, CM3 represents a office LOS environment and CM4 represents an office NLOS environment.

The performance of different estimators are analyzed and compared by calculating the Bit Error Rate (BER) and the Mean Square Error (MSE) that is given by:

$$MSE = ||H - \hat{H}|| \quad (18)$$

Parameters	Specifications
Channel bandwidth	500 MHz
FFT bandwidth	400 MHz
Debit Rate	1 GHz
IFFT/FFT size	256
Number of subcarriers	192
Number of pilot carriers	16
Subcarrier frequency spacing	1.5625 MHz
Type of cyclic prefix	Guard Interval (GI)
Length of cyclic prefix	64
Interpolation method	Linear interpolation (LI)
Constellation	16-QAM
IFFT/FFT period	640 ns
Cyclic prefix duration	160 ns
OFDM symbol period	800 ns
Noise	AWGN
Channel model	CM1, CM3, CM4

TABLE I
OFDM SYSTEM SIMULATION PARAMETERS.

The performance of BER has been compared according to LS and LMMSE under the LOS and NLOS channel environments respectively. From Figure 6, we can see that LMMSE shows better performance than LS.

As shown in Figure 7, the BER under the NLOS channel is higher than that under the LOS channel because the impact of multi-path propagation in the NLOS channel is more significant. For example, we can clearly see that for the LMMSE estimator at a value of SNR = 25 dB, the BER is about $3 \cdot 10^{-1}$, while it was about $2 \cdot 10^{-2}$ in the LOS environment. The same is true for SNR = 40 dB; the BER in the NLOS environment is about 10^{-2} where it is about 10^{-4} in the LOS environment.

In Figure 8, we make a comparison between the two estimates, LS and LMMSE, in another condition of the channel where we are in a residential area in an LOS (i.e. direct visibility) situation.

Note that the performance of the LMMSE algorithm is better than the LS. However, the LMMSE algorithm is less complex.

We can find the same results by comparing MSE, where we note that the LS estimator has a high value of MSE compared to LMMSE. This result is fully compatible with the theory we have set out and explained.

The same results is noted using MSE in figures 10, 11, 12, where the LS estimator has a higher MSE value than the LMMSE estimator. This calculation fully confirm the theory set out and explained in sections IV-C and IV-D.

VI. CONCLUSION

In this study, the estimators LS and LMMSE channel, based on the comb-type pilot technique, are analyzed using

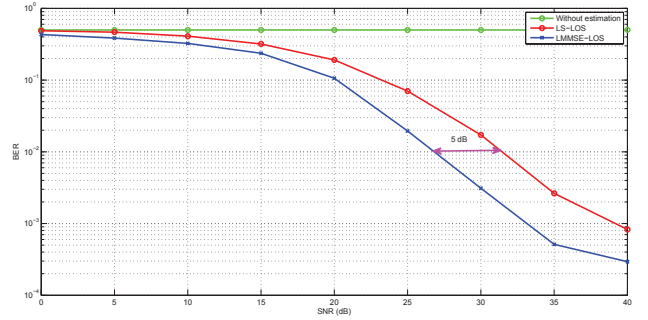


Fig. 6. BER in a LOS environment.

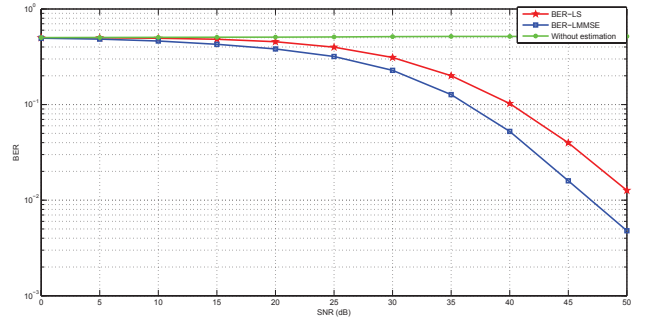


Fig. 7. BER in an NLOS environment.

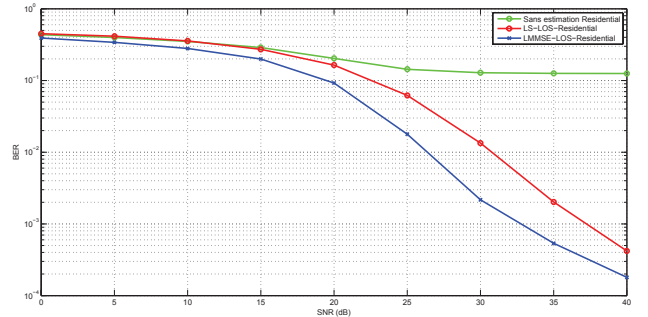


Fig. 8. BER in a residential LOS environment.

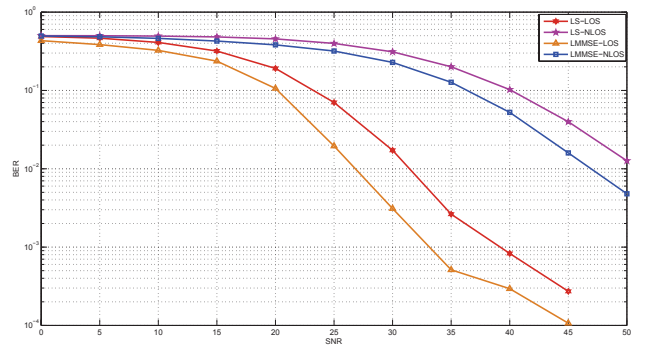


Fig. 9. Comparison between two environments, LOS and NLOS.

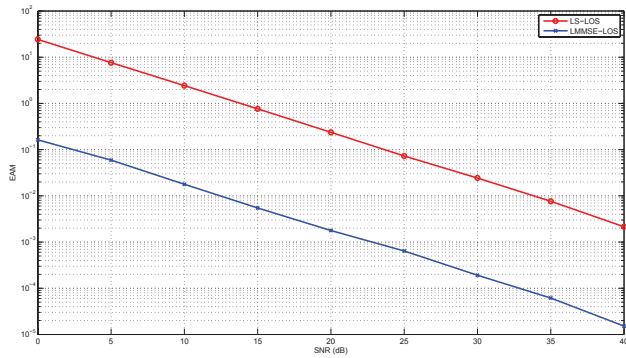


Fig. 10. MSE in an LOS environment.

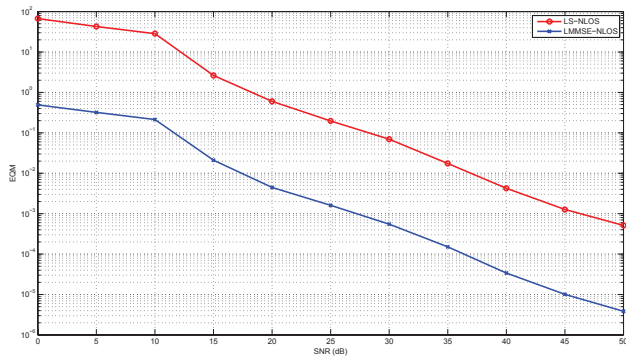


Fig. 11. MSE in an NLOS environment.

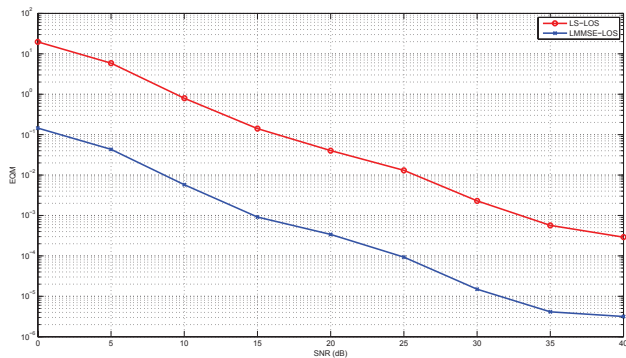


Fig. 12. MSE in a residential LOS environment.

MATLAB simulations under different conditions.

The simulation results show that LMMSE estimation gives better performance but with a higher computational complexity than LS, and that LMMSE has a 5 dB improvement in the LOS case while it offers a 3.5 dB improvement in the NLOS case.

REFERENCES

[1] Van de Beek, J. J., Edfors, O., Sandell, M. et al., "On channel estimation in OFDM systems", vol. 2, July 1995, pages 815-819.

[2] Cimini, L. J., "Analysis and simulation of a digital mobile channel using orthogonal frequency-division multiplexing", 1985, pages 665-675.

[3] Van Nee, R. and Prasad, R. OFDM for Wireless Multimedia Communications. Artech House Publishers, 2000.

[4] Coleri, S., Ergen, M., Puri, A. and Bahai, A., "Channel Estimation Techniques Based on Pilot Arrangement in OFDM Systems", IEEE Transactions on Broadcasting, 48(3) :223-229, septembre 2002.

[5] Saleh, A. A. M., and Valenzuela, R. A. , "A statistical model for indoor multipath propagation", IEEE J. Select. Areas Commun., vol. 5, pp. 128-137, Feb 1987.

[6] Alberto Valdes-Garcia Su-Khiong (SK) Yong, Pengfei Xia. 60 GHz technology for Gbps WLAN and WPAN : from theory to practice. A John Wiley and Sons, Ltd., Publication, 2011..

[7] Mingying Lan, Song Yu, Weilin Li, Wanyi Gu, JianQuan Yao, "A LMMSE Channel Estimator for Coherent Optical OFDM System", IEEE Asia Communications and Photonics, 7632, 2009.

[8] H. Xu, V. Kukshya, T. S. Rappaport, "Spatial and Temporal Characteristics of 60 GHz Indoor Channels", IEEE Journal on Selected Areas in Communications, 20(3) :620-630, April 2002.

[9] X. Ma, H. Kobayashi and S. C. Schwartz, "EM-Based Channel Estimation Algorithms for OFDM", vol. 2004, pages 1460-1477, 2004.

[10] Hussein Hijazi, Laurent Ros, "Polynomial Estimation of Time-Varying Multipath Gains with Inter-carrier Interference Mitigation in OFDM Systems", vol. 58, pages 140-151, January 2009.

[11] Choi, C.-S., Grass, E., Piz, M., Ehrig, M., Marinkovic, M., Kraemer, R. and Scheytt. "60-GHz OFDM systems for multi-gigabit wireless LAN applications", 2010.

[12] Alexander Maltsev et al, Channel models for 60 GHz WLAN systems, IEEE doc. 802.11-09/0334r8, March 2010.

[13] Shen, Y. and Martinez, E., Channel Estimation in OFDM Systems, 2006.